



**HAL**  
open science

## A single stable scheme for steady conjugate heat transfer problems

Marc-Paul Errera, Rocco Moretti, Rami Salem, Yohann Bachelier, Thomas Arrivé, Minh Nguyen

► **To cite this version:**

Marc-Paul Errera, Rocco Moretti, Rami Salem, Yohann Bachelier, Thomas Arrivé, et al.. A single stable scheme for steady conjugate heat transfer problems. *Journal of Computational Physics*, 2019, 394, pp.491-502. 10.1016/j.jcp.2019.05.036 . hal-02502271

**HAL Id: hal-02502271**

**<https://hal.science/hal-02502271>**

Submitted on 9 Mar 2020

**HAL** is a multi-disciplinary open access archive for the deposit and dissemination of scientific research documents, whether they are published or not. The documents may come from teaching and research institutions in France or abroad, or from public or private research centers.

L'archive ouverte pluridisciplinaire **HAL**, est destinée au dépôt et à la diffusion de documents scientifiques de niveau recherche, publiés ou non, émanant des établissements d'enseignement et de recherche français ou étrangers, des laboratoires publics ou privés.

# A Single Stable Scheme For Steady Conjugate Heat Transfer Problems

Marc-Paul Errera <sup>a,\*</sup>, Rocco Moretti <sup>a</sup>, Rami Salem <sup>a</sup>, Yohann Bachelier <sup>a</sup>, Thomas Arrivé <sup>a</sup>, and Minh Nguyen <sup>a</sup>

<sup>a</sup> DAAA, ONERA, Université Paris-Saclay, 29 Avenue de la Division Leclerc, F-92320 - Châtillon, France

**Keywords:** fluid-structure interaction, conjugate heat transfer, thermal coupling, steady, stability

## ABSTRACT

The goal of this paper is to propose a single interface treatment, based on the Dirichlet-Robin interface condition to deal with all steady CHT scenarios. These scenarios depend on the so-called numerical Biot number that controls the stability process and the optimal coefficient that ensures, in theory, unconditional stability. It is shown that this coefficient is closely related to fundamental thermal quantities. For very large thermal fluid-solid interactions, the Dirichlet-Robin condition may result in profound stability issues. A thorough examination of the stability behavior has highlighted a narrow and slow-varying stable zone located around the optimal coefficient. This allows us to determine coupling coefficients valid in any case and the reasonable value of these coefficients avoids significantly impairing the accuracy of CHT solutions. A flat plate, partially protected by a thermal barrier coating, is presented as a test case.

## 1. INTRODUCTION

Conjugate heat transfer (CHT) is a coupled approach that allows to solve complex thermal problems where both structures and flows interact together [1][2]. CHT is one of the fundamental features in a wide range of engineering fluid flow applications. The scope of the CHT analysis could be expanded in the future and systematically employed if robust, reliable, and efficient numerical procedures are implemented. In recent years, the behavior of CHT interface conditions has mainly been studied using a normal mode analysis [3][4][5][6][7]. However, other methods exist to account for the thermal fluid-solid coupling, such as the energy method [8], a matrix analysis [9], a steady-state approach [10], or a frequency-domain method [11]. Currently, the computational cost of a CHT model can be prohibitive if a dynamic coupling process is considered, such as in the context of LES-CHT problems, and different solutions were suggested to accelerate CHT computations [12][13][14][15]. In the current paper, only steady solutions are sought and thus the CHT strategy adopted is such that time consistence is not of concern.

Fluid and solid domains can interact in a variety of ways from low fluid-structure interaction (FSI) characterized by low Biot numbers to high FSI (high Biot numbers). It is well known that for weak/moderate FSI, the Dirichlet-Robin interface condition is well-suited. For higher interactions, another interface treatment must generally be considered. The goal of this paper is to provide a single interface condition that is stable and accurate for all interactions, i.e. regardless of the aero-thermal problem encountered.

Implementing a single interface condition to deal with all situations is extremely interesting. Indeed, the Dirichlet-Robin condition is widely used and it is judicious to be able to extend its application. On the other hand, although it is natural to make use of a Neumann condition when the Biot number is high [10][16], this condition must be implemented according to a criterion that is difficult to estimate. Finally, in the presence of a very heterogeneous surface, for example a metallic wall partially protected by a thermal barrier coating (TBC), one is then confronted with a particularly delicate situation involving a succession of disparate thermal problems much easier to deal with if a single interface condition can be used.

This study is based on the formulation of the optimal coefficient highlighted for the first time in [17]. This concept has proved to be relevant and effective in academic test cases [18] [19] as well as in complex industrial applications [20]. This concept, based on a prototyping study, has provided a foundation for

\* Corresponding author. E-mail address: marc.errera@onera.fr

efficient methods of resolving high interaction thermal coupled problems, as discussed below. The goal of this paper is to define coupling coefficients that never introduce stability restrictions.

## 2. CONJUGATE INTERFACE NUMERICAL METHOD

### 2.1. CHT steady strategy

The simulation of multiphysics problems is generally accomplished by partitioned staggered schemes [21]. In a multiphysics strategy based on a partitioned approach, each system should be treated by the discretization techniques and algorithms that are known to perform well for the single subsystem. As a result, a stable fluid-solid steady solution will be sought by coupling a transient fluid solution with a steady solid state. In this paper, the steady-state Navier-Stokes (laminar or RANS) equations are resolved in the fluid domain and advanced using a time-marching scheme, and a Laplace heat equation is resolved in the solid domain. These strategies, which perform well as single sub-systems, are taken together and assembled in a multiphysics approach. This coupling strategy is thus adopted in this work with a special focus on stability and accuracy issues. Note that this constitutes a traditional loosely-coupled algorithm; the individual physics models are solved independently from one another, and the interface fluxes are balanced only at steady state. However, strong coupling approaches may also be considered to encompass models in which updates are performed together and thus conservation of energy is maintained throughout the whole coupling process [5][22][23].

### 2.2. Dirichlet-Robin interface conditions

Interface conditions are needed on either side of the fluid-structure interface, where coupling conditions are applied. It is well known that Robin conditions have many attractive features and thus a Robin (mixed) condition, currently used in FSI problems [17][24][25][26], is applied on the solid side

$$\left[ \hat{q}_s + \alpha_f \hat{T}_s \right] = \left[ q_f + \alpha_f T_f \right] \quad (1)$$

The subscripts  $f$  and  $s$  denote the fluid and solid domain respectively and the super-imposed hat symbol (^) indicates the sought values.  $q$  is the interfacial heat flux [ $\text{W.m}^{-2}$ ] and  $T$  [K] is the interface temperature. The general Robin condition (1) introduces the coupling parameter  $\alpha_f$  [ $\text{W.m}^{-2}.\text{K}^{-1}$ ] the choice of which directly influences the stability of the CHT process. On the fluid side, a Dirichlet condition is imposed ( $\hat{T}_f = T_s$ ).

### 2.3. Stability analysis

The Godunov-Ryabenkii (G-R) stability analysis [27] is very similar to the standard Fourier stability method, although unlike the Fourier method, the G-R method takes into account the boundary conditions. A normal mode solution is thus applied to the case defined by the discrete model problem [17][18], and after elementary transformations, we obtain the following temporal amplification factor

$$g(z, \alpha_f) = \frac{1}{\beta K_s + \alpha_f} \left[ K_f \cdot \kappa_f(\alpha_f, D_f) + \alpha_f - K_f \right] \quad (2)$$

$K_f$  and  $K_s$  are the fluid and solid conductances respectively [ $\text{W.m}^{-2}.\text{K}^{-1}$ ], that is  $K_f = k_f / \nu \Delta y_f$  ( $\nu = 1/2$  in a finite volume method and  $\nu = 1$  in a finite element method) and  $K_s = k_s / \Lambda_s$ .  $\Delta y_f$  is the size of the fluid cell adjacent to the wall,  $\Lambda_s$  is the solid thickness and  $k$  is the thermal conductivity [ $\text{W.m}^{-1}.\text{K}^{-1}$ ]. Without going into too much detail, let us mention that the parameter  $\beta$  in Eq. (2) accounts for the contributions from the physical and geometric solid characteristics and controls the external boundary condition ( $\beta = 1$ , for a temperature imposed at the external boundary).  $\kappa_f$  is the ‘‘spatial’’ amplification factor that depends on  $\alpha_f$  and on the Fourier number  $D_f$ , expressed by

$$D_f = \frac{a_f \Delta t}{\Delta y_f^2} \quad (3)$$

Where  $a_f$  [ $\text{m}^2 \cdot \text{s}^{-1}$ ] is the thermal diffusivity and  $\Delta t$  [s] is the time step.

#### 2.4. Numerical Biot number

The stability condition  $|g(z, \alpha_f)| < 1$  applied to (2) leads, after some basic calculus manipulations [16] [18], to a lower stability bound  $\alpha_f^{\min}$

$$\alpha_f^{\min} = \frac{K_f}{1 + \sqrt{1 + 2D_f}} - \frac{K_s}{2} \quad (4)$$

This coefficient can be conveniently represented in a shorthand notation

$$\alpha_f^{\min} = \frac{K_s}{2} [Bi_v - 1] \quad (5)$$

This notation introduces the numerical Biot number,  $Bi_v$ , defined by

$$Bi_v = \frac{K_f}{K_s} \left[ \frac{2}{1 + \sqrt{1 + 2D_f}} \right] \quad (6)$$

$Bi_v$  is a local time-dependent parameter that drives the CHT process as long as the fluid may be considered as transient. Note that at steady state ( $D_f = 0$ ), the thermal conductance of the fluid domain shall be taken as the heat transfer coefficient,  $K_f = h$ .

#### 2.5. Weak and strong thermal FSI

Special attention must thus be given to condition (5) from which, one can define :

- **Weak interaction** :  $Bi_v \leq 1$ . If this condition holds, the "transient" thermal resistance of the fluid domain at the shared interface is greater than the resistance offered by the whole solid domain. Note that this "transient" resistance" is strongly influenced by the time step. Accordingly, temperature can be assumed to vary slightly throughout the material's volume. A Dirichlet condition on the fluid side is therefore appropriate. There is no stability restriction.
- **Moderate interaction**  $Bi_v > 1$ . This means that the solid thermal gradients are not negligible or that the thermal fluid conductance is larger than that of the solid. Stability is obtained for  $\alpha_f > \alpha_f^{\min}$ .
- **Strong interaction** :  $Bi_v \gg 1$ . This indicates that either the solid thermal gradients are predominant or that the thermal fluid conductance is much larger than that of the solid (the fluid temperature remains almost the same in the vicinity of the surface). This can lead to a highly non-spatially-uniform temperature field within the solid body. As a result, on a practical level, a Dirichlet condition imposed on the fluid does not seem to provide the most efficient solution. However, we shall see hereafter that this condition can be applied under specific precautions. The stability condition is obtained for a large value of  $\alpha_f$ .

#### 2.6. Optimal coefficient

The modulus of the amplification factor defined by (2) does not have a monotonic variation in terms of  $\alpha_f$ , but goes through an absolute minimum, denoted  $\alpha_f^{opt}$ . At this point, the shape of the curve of the amplification factor switches and turns back as can be seen in Figure 1. Simply stated, the existence of a

transition value for  $\alpha_f$  is identified. This fundamental result was first highlighted in [17]. The amplification factor is represented in Fig. 1 for weak ( $Bi_v = 0.47$ ), moderate ( $Bi_v = 3.03$ ) and strong interaction ( $Bi_v = 7.08$ ). These three different FSI have been obtained easily by varying only the solid thermal conductivity as indicated in Figure 1.

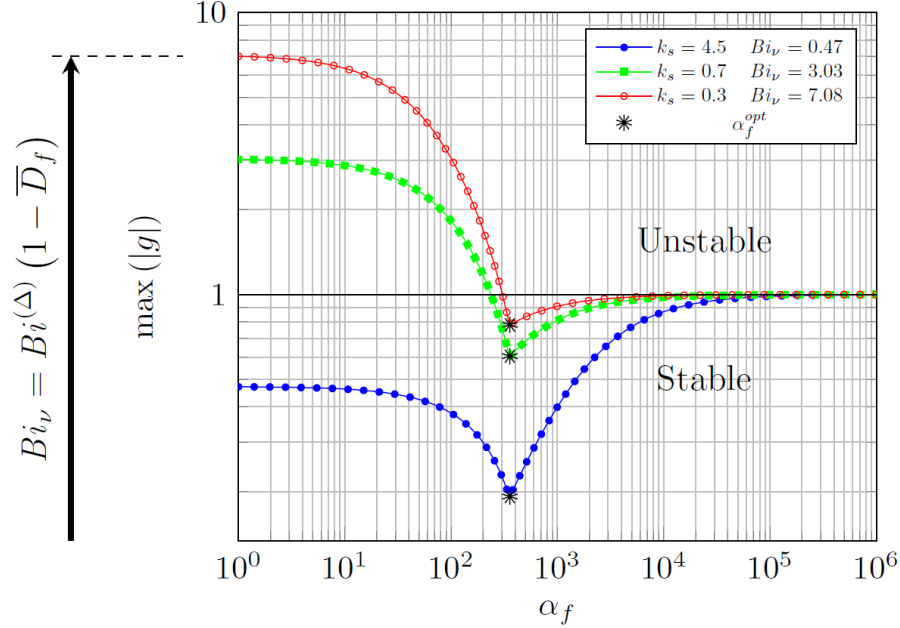


Figure 1 - Amplification factor for three different numerical Biot numbers

The shape of the three curves exhibits a transition when the curves switch and this transition occurs at a unique and remarkable value  $\alpha_f^{opt}$  whose exact expression (see [17], [18] for more details) is given by

$$\alpha_f^{opt} = \frac{k_f}{\nu \Delta y_f} \left[ \frac{1}{1 + \sqrt{1 + 2D_f}} \right] = \frac{K_f}{1 + \sqrt{1 + 2D_f}} \quad (7)$$

When the optimal value defined by (7) is employed, we obtain, in theory, the best-case scenario with no additional computational effort. Note that  $Bi_v$  can also be seen as the y-intercept of the curves in Figure 1.

This number can also be estimated as a function of a normalized Fourier number  $\bar{D}$  [16][18] as indicated in this figure, with

$$(1 - \bar{D}_f) = \frac{2}{1 + \sqrt{1 + 2D_f}} \quad (8)$$

Note that the expression of the optimal coefficient given by Eq.(7) contains only "fluid parameters". This is directly linked with the Dirichlet condition imposed on the fluid side. Indeed, this defines a perfect conducting condition ( $\alpha_s = \infty$ ) and thus totally erases the influence of any "solid parameter" in the definition of  $\alpha_f^{opt}$ .

### 2.7. Optimal coefficient : A link to the penetration depth and to the thermal effusivity

Realistic and accurate thermal conjugate heat transfer solutions require high-resolution CFD meshes. Consequently the placement of the first fluid grid point should fall in the near-wall boundary-layer region, in order to ensure  $y^+$  values close to unity. It is therefore essential to examine, as a first step, the nature of  $\alpha_f^{opt}$

as  $\Delta y_f \rightarrow 0$ . To this regard, contrary to what may seem evident upon examining (7),  $\alpha_f^{opt}$  does not tend to infinity. From (7), we obtain the following limit

$$\alpha_f^{\max} = \lim_{\Delta y_f \rightarrow 0} \alpha_f^{opt} = \frac{k_f}{\nu \Delta y_f} \frac{\Delta y_f}{\sqrt{2a_f \Delta t}} = \frac{k_f}{\nu \sqrt{2a_f \Delta t}} \quad (9)$$

Interestingly enough in (9), the optimal coefficient is inversely proportional to  $\sqrt{2a_f \Delta t}$ , that can be seen as an approximation of the thermal penetration depth or in other words to the diffusion distance, the depth to which the temperature has significantly changed. This shows that for a low penetration, stability must be enhanced by increasing the coupling coefficient to allow for a certain amount of relaxation. Conversely, a large penetration means that more heat is transmitted from the interface to the fluid and this large diffusion naturally translates into a low coupling coefficient.

Another interesting form of (7) can also be obtained

$$\alpha_f^{\max} = \lim_{\Delta y_f \rightarrow 0} \alpha_f^{opt} = \frac{E_f}{\nu \sqrt{2\Delta t}} \quad (10)$$

where  $E_f = \sqrt{k_f \rho C_p}$  [W.s<sup>1/2</sup>/m<sup>2</sup>K] is the thermal effusivity of the fluid. It is the rate at which a medium can absorb heat. This property determines the contact temperature of two bodies that touch each other. It is an interesting fact to note how the optimal coefficient and the thermal effusivity are linked. Seen in this light, one can understand why this coefficient describes the ability of the fluid to exchange heat with the solid at any time in the coupling process. In addition, it should be noted that only the fluid effusivity is present in (10) and not the ratio of the fluid and solid effusivities. As already stated in § 2.6, the Dirichlet condition employed in the current paper (perfect conducting) eliminates any "solid parameter" in the stability analysis.

Finally, it is worth pointing out that the optimal coefficient is a decreasing function of the size  $\Delta y_f$  of the fluid cell. As a result, directly using either (9) or (10) in any CHT case, regardless of the cell size  $\Delta y_f$ , presents an obvious possibility that avoids the necessity of estimating the length of the cell. This is true as long as the near-wall treatment is based on a low-Reynolds modeling. In this case, we may consider that  $\alpha_f^{\max}$  is very close to  $\alpha_f^{opt}$ , and thus,  $\alpha_f^{\max}$  can be used directly as is. This will lead to a very slight overestimation (in general,  $\alpha_f^{\max} \approx 1.1 \alpha_f^{opt}$ ) of the value of  $\alpha_f^{opt}$ , which does not adversely affect stability.

## 2.8. Nature of the thermal FSI

At low or moderate interaction, there is no stability issue when a Dirichlet-Robin is employed. However, a good choice of the coupling coefficient is needed. Figure 2 displays the temperature profile at the leading edge of a flat plate in a CHT computation (see details in [16]). Two coupling coefficients have been used :  $\alpha_f = 0.61 * \alpha_f^{opt}$  and  $\alpha_f = \alpha_f^{opt}$ . The numerical Biot number is  $Bi_\nu \approx 26$ .

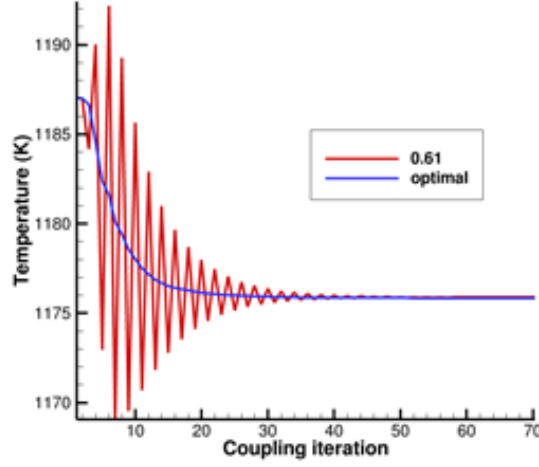


Figure 2 - Convergence history for two coupling coefficients.

It is clear from this figure that  $\alpha_f = 0.61 * \alpha_f^{opt}$  generates oscillations during the initial coupling steps. The oscillations tend to grow at the beginning. Although the amplitude of these oscillations does not exceed 2%, they can become a critical issue if they do not decrease rapidly. Finally, we can see that the oscillations die out after approximately 40 fluid-solid coupling periods, indicating that the coupling coefficient is too low and consequently producing under-relaxed solutions. On the contrary, the choice of  $\alpha_f = \alpha_f^{opt}$  avoids all oscillations, and a monotonic behavior can be observed even during the particularly difficult initial instants. An oscillatory behavior can ultimately lead to a divergent process, and thus these oscillations must be avoided at all costs.

In the region  $\alpha_f < \alpha_f^{opt}$ , the amplification factor is a decreasing function of  $\alpha_f$ , as shown in Figure 1. It is a time-dependent hyperbola that strongly relies on the Fourier number  $D_f$ . This dependence can lead to serious stability problems. As  $D_f$  decreases, the amplification factor increases. In the region  $[\alpha_f^{min}, \alpha_f^{opt}]$ , the CHT problem is theoretically stable but oscillations may occur as shown in Figure 2. It is therefore absolutely necessary to further limit the range of  $\alpha_f$  to avoid adopting a coupling coefficient in this zone, even if  $\alpha_f = \alpha_f^{opt}$  theoretically leads to a monotone and fast convergence as predicted by the stability analysis. However, the problem becomes even more significant if thermal interactions are strong, as shown below.

### 2.9. Biot number and numerical Biot number

Let us recall that the conventional Biot number needs a heat transfer coefficient,  $h$

$$Bi = \frac{h}{K_s} \quad (11)$$

This number is a key parameter that determines the stability of the fluid-solid equilibrium and the conditions for relevant transmission procedures, see Verstraete *et al.* [10][26]. It is not an easy task to set up a coupling method on the basis of the conventional Biot number if fluid transients are involved in the coupling process. However, at convergence, stability bounds may be expressed as a function of this number.

The numerical Biot number is a dimensionless number introduced by Eq.(6), and is defined at any time in the transient state of a CHT computation. It is the result of a balance between the fluid and solid domains. It can also be expressed quite simply

$$Bi_v = \frac{2\alpha_f^{opt}}{K_s} \quad (12)$$

It is a key parameter for stability since it measures the strength of the fluid-solid thermal interaction, and accounts for the transient fluid flow at the interface. This number controls the stability process and guides the interface condition choice. Note that the expressions of (11) and (12) have the same denominator. The first number represents the steady fluid-solid equilibrium while the second is defined during the transient processes.

As for the optimal coefficient, an upper bound of  $Bi_v$  is given for  $\Delta y_f = 0$

$$Bi_v^{\max} = \lim_{\Delta y_f \rightarrow 0} Bi_v = \frac{k_f}{k_s} \frac{2\Lambda_s}{v\sqrt{2a_f\Delta t}} \quad (13)$$

As  $Bi_v$  is a decreasing function of  $\Delta y_f$ ,  $Bi_v^{\max} < 1 \Rightarrow Bi_v < 1$ . As a result, it is an easy matter from (13) to determine any quantity that ensures unconditional stability, i.e. a large diffusion of heat in the fluid domain from the interface, which can be characterized by a weak thermal FSI, as defined in Section 2.5. However, this is an aside, as the goal of this work is to prioritise very large FSI.

Finally, let us recall that it was shown recently [19] that for stability reasons, the following condition in the fluid domain, must be verified to avoid a "spatial" exponential growth of  $\kappa_f$  in Eq.(2):

$$K_f > \frac{h}{2} \quad (14)$$

This stability condition indicates that the fluid conductance in the near-wall region (diffusion) must be higher than half of the convective heat transfer coefficient. Clearly, this condition holds in the vast majority of situations in the fluid. However, this relationship should not be overlooked when the heat transfer coefficient is expected to be very high (in the case of an impinging jet, for instance).

### 3. A SINGLE INTERFACE TREATMENT : A STABILITY CHALLENGE

#### 3.1. Strong thermal interaction

It is the purpose of this article to propose a single interface treatment, based on the Dirichlet-Robin condition. Why this condition in particular ? First, because it is the most widely used in CHT computations. Second, because the numerical Biot number can be lowered thanks to the temporal term  $\left[1 + \sqrt{1 + 2D_f}\right]^{-1}$ , presenting a powerful argument in favor of the Dirichlet condition. It is the reason why, only this condition will be used in the current paper.

As mentioned before, a Dirichlet condition imposed on the fluid side may be delicate and difficult for stability in the case of very strong thermal interactions ( $Bi_v \gg 1$ ). Nevertheless, one can also argue that the optimal coefficient provides, even in this case, unconditionally stable CHT computations. However, this result has been obtained from a 1D model and, unfortunately, at very strong thermal interactions, the optimal value becomes very close to the stability limit. This can easily be shown. Combining the definition of  $\alpha_f^{\min}$  (Eq. (5)) and  $\alpha_f^{\text{opt}}$  (Eq. (7)), we obtain

$$\frac{\alpha_f^{\text{opt}} - \alpha_f^{\min}}{\alpha_f^{\text{opt}}} = \frac{1}{Bi_v} \quad (15)$$

Thus, as  $Bi_v$  increases, two undesirable consequences are observed : the interval  $[\alpha_f^{\min}, \alpha_f^{\text{opt}}]$  shrinks rapidly, and the amplification factor approaches unity.



In summary,  $Bi_v$  measures the strength of the thermal FSI (y-intercept in Figure 1) and  $Bi_v^{-1}$  is the distance between  $\alpha_f^{opt}$  and the unstable zone (relative distance along the x-axis).

### 3.2. A stable slow-varying zone

It is now useful to intensively examine the influence of the coupling coefficient on convergence by scanning a field for  $\alpha_f$  from 0 (no negative values are admitted for stability reasons) to  $K_f$ . The curve in Figure 3 shows the number of coupling iterations necessary to converge (to a specified tolerance), as a function of the coupling coefficient. Each point of the curves indicates a converged CHT computation. The convergence criterion is based on the infinity norm of the absolute interface temperature  $\Delta T_f$ . Three tolerances have been adopted ( $\varepsilon = 10^{-2}; 10^{-5}; 10^{-8}$ ). All the curves show a divergence up until or rather shortly after  $\alpha_f^{min}$ , after which a strong decay can be seen. Interestingly, in each case, a stable minimum level around  $\alpha_f^{opt}$  is observed, characterized by a slight slope. After this nearly flat zone, this slope increases abruptly after  $3 \cdot \alpha_f^{opt}$ , indicating a sudden decrease in the speed of the convergence. Accordingly, we should make use of the potential of this narrow slow-varying zone  $[\alpha_f^{opt}, 3 \alpha_f^{opt}]$  to guarantee stable and fast coupled computations for all cases.

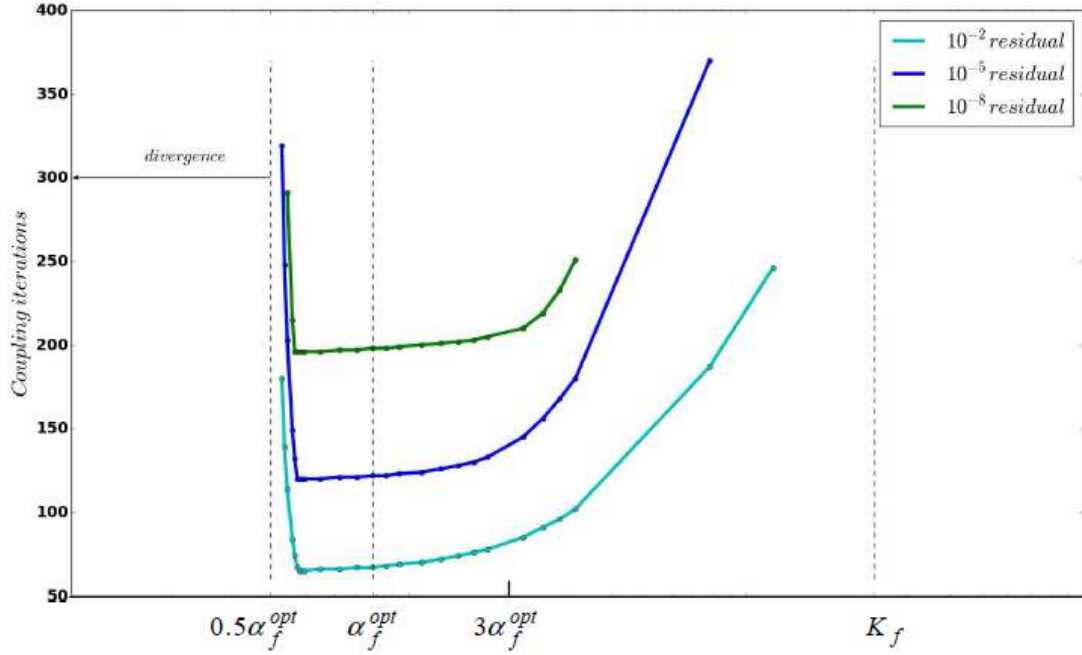


Figure 3 - Coupling iterations to converge for 3 different tolerances.

Beyond the limit  $3 \cdot \alpha_f^{opt}$ , the CHT process is slowed down uselessly. The existence of this flat stability zone which varies little with  $\alpha_f$ , as illustrated if Fig.3, provides a range of values for  $\alpha_f$  that resolves the problem presented by a very large numerical Biot number, brought to light by Eq.(15).

### 3.3. Stability conditions for very strong thermal interactions

On the basis of the above, it is clear that the coupling coefficient must be chosen such that  $\alpha_f \leq 3 \alpha_f^{opt}$ , since large values of  $\alpha_f$  ensure stability but lead to needlessly long calculations. Let us recall [18] that the

amplification factor for  $\alpha_f \geq \alpha_f^{opt}$ , always located in the stable zone, is a time-independent hyperbola whose equation is

$$g(\alpha_f) = \frac{\alpha_f}{K_s + \alpha_f} \quad (16)$$

As can be seen from Figure 1, the slope of the right half-curve is very steep at  $\alpha_f = \alpha_f^{opt}$ . The right-derivative of  $g(\alpha_f)$  is given by

$$g'(\alpha_f) = \frac{K_s}{(K_s + \alpha_f)^2} \quad (17)$$

When the interval  $[\alpha_f^{opt}, \alpha_f]$  is too small, the risk of instability remains high. Systematic numerical investigations have revealed that when the slope of the right-hand side becomes three times lower, the distance  $|\alpha_f - \alpha_f^{opt}|$  becomes sufficiently large and any risk of instability is avoided. Thus,  $\alpha_f$  must be determined such that the slope of the amplification factor is at least three times lower than that of the optimal coefficient. This translates to the requirement

$$\frac{K_s}{(K_s + \alpha_f)^2} \leq \frac{1}{3} \frac{K_s}{(K_s + \alpha_f^{opt})^2} \quad (18)$$

Whence

$$3(K_s + \alpha_f^{opt})^2 \leq (K_s + \alpha_f)^2 \quad (19)$$

The issue at hand is with regard to very strong thermal interactions, i.e.,  $Bi_v \gg 1$ , which implies  $\alpha_f^{opt}/K_s \gg 1$ . Thus, (19) becomes

$$\alpha_f > \sqrt{3} \alpha_f^{opt} \quad (20)$$

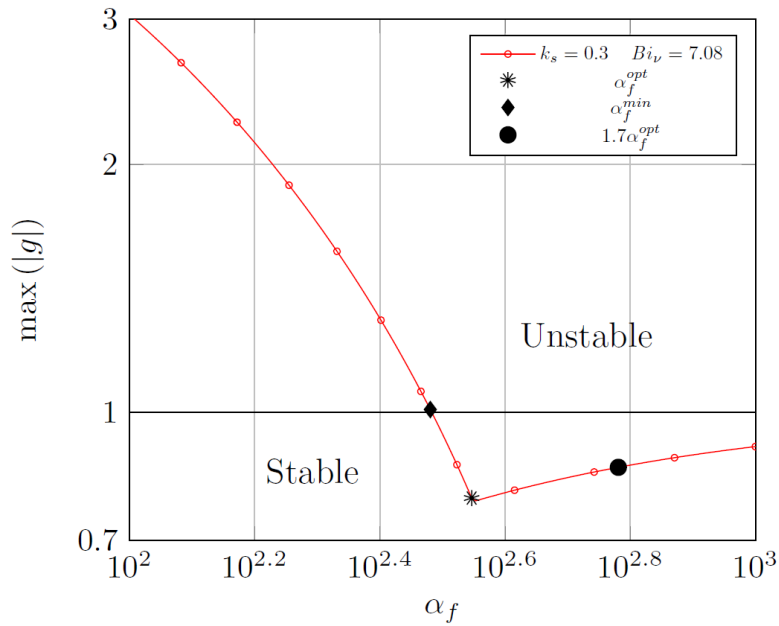


Figure 4 - Zoomed view of the amplification factor.

Figure 4 shows a zoomed view of the amplification factor and the position of  $\alpha_f^{\min}$ ,  $\alpha_f^{\text{opt}}$ , and  $\sqrt{3} \alpha_f^{\text{opt}}$ .

### 3.4. A significant example

Figure 5 has been obtained in the conjugate case generated for testing and demonstrating the efficiency of the optimal coefficients. This figure illustrates the convergence history for various values of the coupling coefficient by plotting the interface temperature residuals as a function of the coupling coefficient.

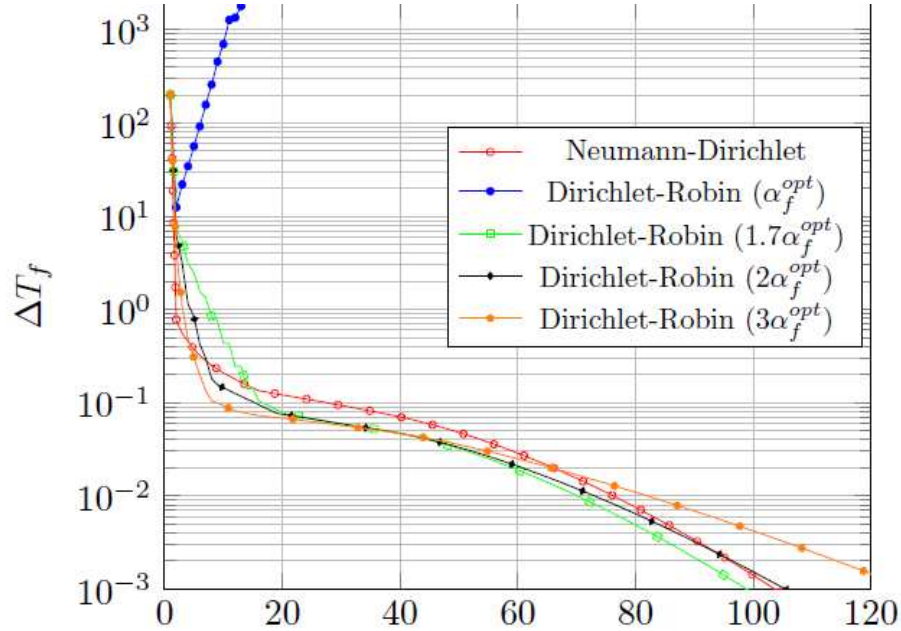


Figure 5 - Convergence vs coupling iterations for Dirichlet-Robin & Neumann-Dirichlet conditions.

The details of the CHT test case are provided in [16]. It is quite interesting to mention that the results of the figure were obtained for a very high numerical Biot number  $Bi_v = 428.$ , due to a very low solid conductivity ( $k_s = 10^{-2}$ ).

In [16], only the Dirichlet-Robin (with the optimal coefficient) and the Neumann-Robin conditions were shown. As we can see, the first condition is divergent while the second converges rapidly (104 coupling iterations are needed). However, we have now introduced the coefficients provided by the current study, namely condition (20) with an upper limit of  $\alpha_f < 3 \alpha_f^{\text{opt}}$ . For  $\alpha_f = \sqrt{3} \alpha_f^{\text{opt}}$ , a rapidly convergent behavior is observed (99 coupling iterations) which suggests that this coefficient provides an efficient condition. However a small non-uniform behavior is detected since an obvious "step-off" is noted in the initial coupling steps. The other two coefficients lead to oscillation-free solutions but at a slightly larger cost (106 iterations and 127 iterations, respectively). Values greater than  $3 \alpha_f^{\text{opt}}$  are acceptable, albeit at the cost of a poor convergence rate.

Note that such a high numerical Biot number seldom or never occurs, as the solid conductivity used is 100 times smaller than that of typical ceramics ! It is the reason why Figure 5 is entirely representative of extreme CHT cases.

### 3.5. Computational efficiency

The number of fluid iterations necessary to converge must be compared to that for an uncoupled steady flow solution. For low or moderate fluid-structure interactions, it has been shown [16] that the number of

fluid iterations of the CHT process is shorter than the one required for a CFD computation only. At very high interactions, such as the one shown in Figure 5, the number of fluid iterations increases by only 15% with respect to the CFD computation.

### 3.6. Stability, accuracy and validation

Emphasis has been put in this paper on stability issues, mainly for large thermal fluid-structure interactions. This was a necessary step to complete before dealing with accuracy issues such as how the numerical treatment at the interface affects the overall spatial convergence and accuracy. However, in loosely coupled problems, the heat fluxes are not balanced at the interface and only a steady state is sought. On the contrary, in strong thermal coupling, conservation of energy must be maintained continuously. Note that, for this specific issue, the method of manufactured solutions [28][29] has been used by Veeraragavan *et al.* to verify that the spatial discretisation used at the fluid-solid interface does not affect the overall spatial convergence and that the coupling is implemented correctly. Lastly, it should be observed that there are few analytical solutions. They are available only for simple cases with linear boundary conditions. For incompressible flows, analytical solutions have already been used in CHT for instance in a parallel plate duct [30] [31], in circular ducts [31], with periodic inlet fluid temperature [32] or in laminar pipe flows [33]. For compressible flows, no exact solution is available.

## **4. A SINGLE INTERFACE TREATMENT : AN ACCURACY CHALLENGE**

### 4.1. Background

In theory, the convergence of the conjugate problem implies the continuity of temperature and heat flux at the fluid-solid interface : introducing the continuity of temperature  $T_f = T_s$  into the Robin condition (1) leads to  $q_f = q_s$ . In practice, the situation can be quite different. The problem is twofold :

(1) the interface conditions are satisfied to a specified tolerance  $\varepsilon$  :

$$|T_f - T_s| < \varepsilon \quad (21)$$

(2) The "relaxation term" in (1), namely  $\alpha_f (T_f - T_s)$ , may be significant. This term, which is meant to tend towards zero at convergence, may, on the contrary, have significant influence on the solution. Indeed, it can be of equal or greater order of magnitude as  $q_f$ , leading to an erroneously converged result.

At this stage, it is worth noting that a criterion based on the difference between the fluid and solid heat fluxes could have been considered, but this would have led to quite similar conclusions. Indeed, from Eq.(1), we obtain

$$q_s - q_f = \alpha_f (T_f - T_s) \quad (22)$$

and thus, when criterion (21) holds, the convergence error on the heat fluxes is

$$|q_s - q_f| \approx \alpha_f \cdot \varepsilon \quad (23)$$

Therefore, this difference is all the more important when the coupling coefficient is large (strong thermal interactions) or when the tolerance criterion is not restrictive enough.

### 4.2. Non-Uniqueness of the CHT solutions

On a discrete level, on the solid side, at time  $n+1$ , it is not Eq.(22) that is solved but rather :

$$q_s^{n+1} = \tilde{q}_f^n + \alpha_f (\tilde{T}_f^n - T_s^{n+1}) \quad (24)$$

where  $\tilde{q}_f$  and  $\tilde{T}_f$  are the spatially interpolated values from the fluid grid to the solid grid. This may be rewritten as :

$$q_s^{n+1} = \tilde{q}_f^n + \alpha_f (T_s^n - T_s^{n+1}) + \alpha_f (\tilde{T}_f^n - T_s^n) \quad (25)$$

And thus, as we can see, convergence on the solid side ( $T_s^{n+1} = T_s^n$ ), does not imply continuity of heat flux ( $q_s^{n+1} = \tilde{q}_f^n$ ), due to the interpolated fluid temperature. This convergence error is accentuated as thermal interactions get stronger, since increasingly large coupling coefficients become necessary. Consequently, a single interface treatment based on a Dirichlet-Robin condition presents a real accuracy challenge. All this upholds the necessity of a coupling coefficient that remains close to  $\alpha_f^{opt}$  in the case of high thermal FSI. The test case, presented in Section 4, illustrates that a family of solutions can be obtained at large thermal fluid-solid interaction.

As a result, in the framework of the Dirichlet-Robin condition, the interpolation error can be substantially reduced if only one thermal quantity - the heat flux - is interpolated at the shared interface. In this way, there is no need to transfer the fluid temperature to the solid and the relaxation term is simply taken as  $\alpha_f (T_s^n - T_s^{n+1})$ . This has a minor influence in the case of low numerical Biot numbers where small or zero coupling coefficients are acceptable, but it is vital when higher thermal interactions are considered.

### 4.3. TBC test case

#### 4.3.1. Operating conditions

Figure 6 shows a 300 mm long and 9.8 mm thick rectangular flat plate with a thermal conductivity  $k_s = 10 \text{ Wm}^{-1}\text{k}^{-1}$ . The CHT analysis consists of the problem of convective heat transfer over, and conductive heat transfer within, this plate. The upper face of the plate is partially protected by a ceramic thermal barrier coating (a ceramic of 0.2  $\mu\text{m}$  thickness from probe 2 to probe 3-  $k_{TBC} = 0.1 \text{ Wm}^{-1}\text{k}^{-1}$ ). The external faces of the solid plate ( $k_s = 10 \text{ Wm}^{-1}\text{k}^{-1}$ ) are assumed to be adiabatic and a constant temperature (1000 K) is imposed on the lower side of the solid. The solid contains 22 mesh-points uniformly distributed in the y-direction.



Figure 6 - Thermal barrier coating on a flat plate.

The fluid domain is a rectangular channel of the same length as the solid plate with a symmetry boundary condition on the upper side. Turbulent air flows from the inlet and interacts with the upper wall of the solid before exiting. A near wall well-refined mesh ( $\Delta y_f = 2.5 \cdot 10^{-5} \text{ m} - y^+ \sim 1$ ) is employed to correctly capture the boundary layer. This allows us to best calculate the heat transfer and as a result, no wall functions are employed. The fluid Mach number is 0.1 and the total temperature is 1200 K. The CFL is set at 20. The figure indicates the position of four probes.

#### 4.3.2. Numerical tools

The fluid code, referred to as the *elsA* software package (ONERA-Airbus-Safran property), is a multi-purpose tool for applied aerodynamics and multi-physics, which capitalizes on the innovative results of CFD research [34][35]. The solid software package, called Z-set, is a comprehensive suite of integrated analysis

programs for general purpose structural analysis [36]. The exchange of data between the two aforementioned solvers is carried out through the CWIPI library [37]. This library takes into account the grids, as well as the processes in which the data are located.

#### 4.3.3. Results

The converged interface temperature, within a specified tolerance  $\varepsilon = 10^{-5}$ , is represented vs the coupling coefficient in Figure 7. Along the  $x$ -axis, the indices 1, 2, etc ...represent  $1.*\alpha_f^{opt}$ ,  $2.*\alpha_f^{opt}$ , etc. The value of the thermal conductivity of the TBC and of the solid body is indicated in this figure.

It can be seen that the temperature levels at probes 1 and 4, i.e. in the metallic body, are independent of the coupling coefficient. On the contrary, at the two boundaries between the metal and the TBC, the coefficient-dependency on the steady coupled solution is evident and notable differences can be observed despite the very low tolerance level required. This confirms what one would expect. It is more difficult to obtain good convergence properties with a small solid thermal conductivity when a temperature is prescribed on the fluid side.

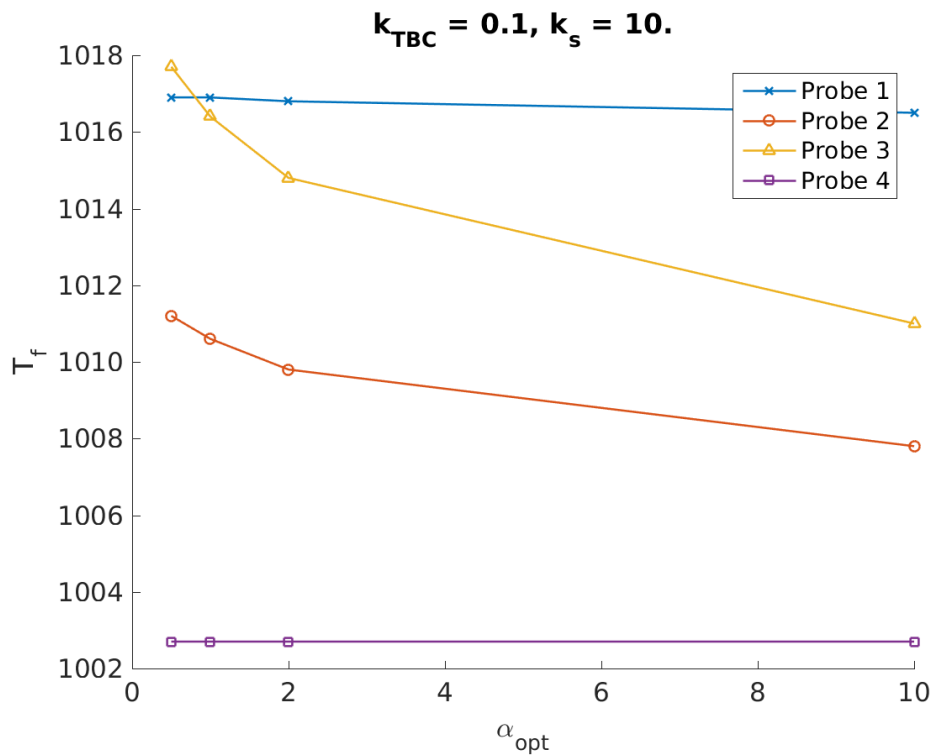


Figure 7 - Interface temperature at convergence at 4 different locations vs coupling coefficient.

At this point, it is essential to illustrate the convergence of the temperature for the different coefficients. As can be seen from Figure 7, temperature at Probe 1 and Probe 2 are not affected by the value of the coupling coefficient. This does not hold true when the numerical Biot number is large, as in the case of the probes by the thermal coating. Consequently, the convergence history of the temperature is shown in the TBC at probe 3.

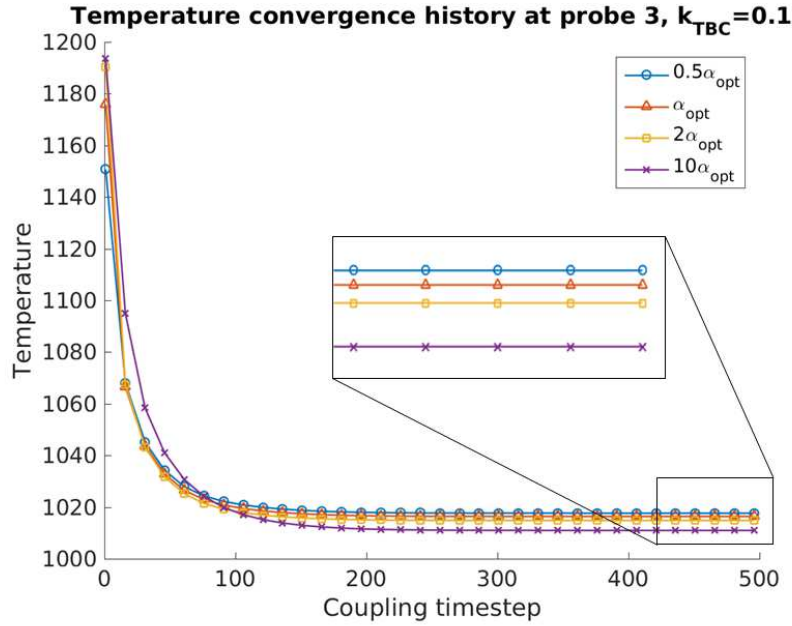


Figure 8 - Interface temperature at convergence at probe 3, for different coupling coefficients.

The variation in the solutions at steady state cannot be considered to be negligible, as the difference in temperature can be as large as 8 K when considering the lowest and largest coefficients. As explained in Section 4.2, these non-unique solutions are due to the relaxation term that becomes predominant with strong FSI. It is then crucial to specify that if the relaxation term contains only "solid temperatures", as suggested before, all the interface temperatures presented in Figure 8, for 4 coupling coefficients, are superimposed, which means that a unique solution is obtained.

Finally, it is highly significant to note that a Neumann-Dirichlet condition imposed at the TBC interface (between probes 2 and 3) and a Dirichlet-Robin condition imposed in the rest of the interface lead to a rapidly divergent process (not shown in this paper). This is because switching from a Dirichlet-type condition ( $\alpha_s = \infty$ ) to a Neumann condition ( $\alpha_s = 0$ ) is very brutal. It is thus far better to implement, at least in the case in point, a single interface condition. This fully justifies the approach presented in the current study.

## 5. CONCLUSION

A single interface treatment to deal with all steady CHT scenarios has been presented in this paper. This treatment is based on adaptive and local coupling coefficients, with no arbitrary relaxation parameters, and with no assumptions on the temporal advancement of the fluid domain. This was achieved by leveraging the concept of optimal coupling coefficients and by extending their functionalities to include high thermal FSI.

Accordingly, stability is maintained in any CHT event, and in particular for a thermal coupling characterized by very large Biot numbers. In addition, it has been shown how this approach is closely related to the thermal effusivity as well as the thermal penetration depth, making this interface treatment a highly physics-based approach. Finally, in order to avoid significantly impairing the accuracy of a CHT solution, a reasonable range of values for the coupling coefficient has been stressed. However, we must also bear in mind that the time step involved in the CHT analysis is a significant variable in the stability model. This procedure could thus be generalized by calculating the optimal coefficient with a diffusion time scale. The most direct application under study consists in heterogeneous coupled surfaces, such as a metallic wall partially protected by a thermal barrier coating.

## ACKNOWLEDGEMENT

The authors would like to acknowledge the "Direction Scientifique Générale" of ONERA for providing a support for this work. The studies presented in this article make use of elsA-ONERA, a software package jointly owned by Airbus, Safran, and ONERA.

## 6. REFERENCES

- [1] T.L. Perelman, On conjugated problems of heat transfer. *International of Journal Heat and Mass Transfer*, 3 (1961) 293-303.
- [2] A. Dorfman, Z. Renner, Conjugate Problems in Convective Heat Transfer : Review, *Mathematical Problems in Engineering*. (2009) Article ID 927350.
- [3] M.B. Giles, Stability Analysis of Numerical Interface Conditions in Fluid-Structure Thermal Analysis, *International Journal for Numerical Methods in Fluids*, 25, pp. 421-436, 1997.
- [4] B. Roe, R. Jaiman, A. Haselbacher, and P.H. Geubelle, Combined interface boundary method for coupled thermal simulations, *Int. J. Numer. Meth. Fluids* 57, pp. 329-354, 2008.
- [5] W.D. Henshaw, and K.K. Chand, A composite grid solver for conjugate heat transfer in fluid-structure systems, *Journal of Computational Physics* 228, pp 3708-3741, 2009.
- [6] V. Kazemi-Kamyab, A.H. van Zuijlen, and H. Bijl, Accuracy and stability analysis of a second-order time-accurate loosely coupled partitioned algorithm for transient conjugate heat transfer problems, *Int. J. Numer. Meth. Fluids*, DOI: 10.1002/flid.3842, 2013.
- [7] O. Joshi and P. Leyland, Stability Analysis of a Partitioned Fluid-Structure Thermal Coupling Algorithm, *Journal of Thermophysics and Heat Transfer*, Vol. 28, N°1, January-March 2014.
- [8] J. Lindström, and J. Nordström, A stable and high-order conjugate heat transfer problem, *Journal of Computational Physics* 229, pp 5440-5456, 2010.
- [9] F.-X. Roux, and J.-D. Garaud, Domain Decomposition Methods Methodology with Robin Interface Matching Conditions for Solving Strongly Coupled Fluid-Structure Problems, *International Journal for Multiscale Computational Engineering*, 7, Issue 1, pp. 9-16, 2009.
- [10] T. Verstraete and S. Scholl, Stability analysis of partitioned methods for predicting conjugate heat transfer, *International Journal of Heat and Mass Transfer*, 2016, 101, 852-869.
- [11] L. He and M.L.G. Oldfield, Unsteady conjugate heat transfer modeling, *Journal of Turbomachinery*, Vol. 133, N°3, 2011.
- [12] F. Duchaine, A. Corpron, L. Pons, V. Moureau, F. Nicoud, T. Poinot, Development and Assessment of a Coupled Strategy for Conjugate Heat Transfer with Large Eddy Simulation: Application to a Cooled Turbine Blade, *Int. J. Heat Fluid Flow*, 30(6), pp.1129–1141, 2009.
- [13] S. Jaure, F. Duchaine, G. Staffelbach and L.Y.M Gicquel, Massively parallel Conjugate Heat Transfer Methods relying on Large Eddy Simulation applied to an Aeronautical Combustor, *Computational Science & Discovery* 6 (2013) 015008, 2013.
- [14] L. He and M. Fadhil, Multi-scale time integration for transient conjugate heat transfer, *International Journal for Numerical Methods in Fluids*, Vol. 83, 12, pp 887-904, 2016.
- [15] C. Koren, R. Vicquelin, O. Gicquel, Self-adaptive coupling frequency for unsteady coupled conjugate heat transfer simulations, *International Journal of Thermal Sciences*, 2017, 118, pp.340- 354.
- [16] R. Moretti, M.-P. Errera, V. Couaillier, F. Feyel, Stability, convergence and optimization of interface treatments in weak and strong thermal fluid-structure interaction, *International Journal of Thermal Sciences*, 126, pp 23-37, 2018.
- [17] M.-P. Errera and S. Chemin, Optimal solutions of numerical interface conditions in fluid-structure thermal analysis, *Journal of Computational Physics*, 2013, 245, pp 431-455.
- [18] M.-P. Errera and F. Duchaine, Comparative study of coupling coefficients in Dirichlet-Robin procedure for fluid-structure aerothermal simulations, *Journal of Computational Physics*, 2016, 312, 218-234.
- [19] M.-P. Errera, M. Lazareff, J.-D. Garaud, T. Soubrié, C. Douta, T. Federici, A coupling approach to modeling heat transfer during a full transient flight cycle. *International Journal of Heat and Mass Transfer*, April 2017.



- [20] R. El Khoury, M. Errera, K. El Khoury, M. Nemer, Efficiency of coupling schemes for the treatment of steady state fluid-structure thermal interactions. *International Journal of Thermal Sciences*, 115 (2017) 225-235.
- [21] C.A. Felippa and K.C. Park, Staggered transient analysis procedures for coupled dynamic systems: formulation. *Computer Methods in Applied Mechanics and Engineering*, 1980, 24:61-1.
- [22] A. Veeraragavan, J. Beri and R.J Gollan, Use of the method of manufactured solutions for the verification of conjugate heat transfer solvers. *Journal of Computational Physics*, <https://doi.org/10.1016/j.jcp.2015.12.004>, 2015.
- [23] F. Meng, S. Dong, J. Wang and D. Guo, A new algorithm of global tightly-coupled transient heat transfer based on quasi-steady flow to the conjugate heat transfer problem, *Theoretical and Applied Mechanics Letters*, Volume 6, Issue 5, September 2016, Pages 233-235
- [24] S. Badia, F. Nobile, C. Vergara, Fluid-structure partitioned procedures based on Robin transmission conditions, *Journal of Computational Physics* 227 (14) (2008) 7027-7051.
- [25] J.W. Banks, W.D. Henshaw, D.W. Schwendeman, An analysis of new stable partitioned algorithm for FSI problems. Part 1 : Incompressible flow and elastic solid, *Journal of Computational Physics* 269 (2014) 108-137.
- [26] S. Scholl, B. Janssens, T. Verstraete, Stability of static conjugate heat transfer coupling approaches using Robin interface conditions. *Computers & Fluids*, Vol.172, pp 209-225, 2018.
- [27] SK. Godunov and VS. Ryabenkii, The theory of difference schemes. An introduction. North-Holland: Amsterdam, 1964.
- [28] S. Steinberg, P.J. Roache, Symbolic manipulation and computational fluid dynamics, *Journal of Computational Physics* 57 (2) pp 251-284, 1985.
- [29] C.J. Roy, Review of code and solution verification procedures for computational simulation, *Journal of Computational Physics* 205 (1) pp 131-156, 2005.
- [30] J. Susec, Exact solution for unsteady conjugated heat transfer in the thermal entrance region of a duct, *Journal of Heat Transfer* 109(2), 295-299, 1987.
- [31] M.A. Al-Nimr and M.A.I. Al-Shaarawi, Analytical solutions for transient conjugated heat transfer in parallel plate and circular ducts. *Int. Comm. Heat Mass Transfer*, 19, pp 869-878, 1992.
- [32] J.S. Travelho and W.F.N. Santos, Solution for transient conjugated forced convection in the thermal entrance region of a duct with periodically varying inlet temperature, *Trans. ASME J. Heat Transfer* 113 (1991) 558–562.
- [33] S. Olek, E. Elias, E. Wacholder, and S. Kaizerman, Unsteady conjugated heat transfer in laminar pipe flow, *Int. J. Heat Mass Transfer* 34 (1991) 1443–1450.
- [34] L. Cambier, S. Heib, and S. Plot, "The Onera elsA CFD software: input from research and feedback from industry," *Mechanics & Industry*, Vol.14, N°3, 2013, pp 159-174.
- [35] <http://elsa.onera.fr/>
- [36] <http://www.zset-software.com>
- [37] <http://sites.onera.fr/cwipi/>